Phys. Status Solidi C 9, No. 6, 1496–1498 (2012) / DOI 10.1002/pssc.201100766

physica status solidi c
www.pss-c.com
current topics in solid state physics

Electroluminescence from amorphous silicon/crystalline silicon solar cells and its temperature dependence

Rudolf Brüggemann *

Institut für Physik, Carl von Ossietzky Universität Oldenburg, 26111 Oldenburg, Germany

Received 25 October 2011, revised 23 January 2012, accepted 29 January 2012
Published online 26 April 2012

Keywords electroluminescence, heterojunction, interface defects, silicon solar cell

* e-mail rudi.brueggemann@uni-oldenburg.de, Phone: +49 441 798 3497, Fax: +49 441 798 3201

The quality of the amorphous silicon/crystalline silicon interface is decisive for efficient operation of amorphous silicon/crystalline silicon heterojunction solar cells. We investigate the electroluminescence from these heterojunction solar cells for a variation of interface properties. We detail electroluminescence results from temperature-dependent simulations which show that the electroluminescence yield at constant current density is almost temperature-independent for lower interface-defect densities while for higher interface-defect densities the electroluminescence yield decreases with decreasing temperature. In contrast to the influence of the front interface which does not change the spectral shape, the related inhomogeneous carrier profile distorts the spectrum so that conclusions can be drawn on the rear interface properties.

1 Introduction Hydrogenated amorphous silicon – crystalline silicon (a-Si:H/c-Si) heterojunction solar cells are formed by thin doped and undoped a-Si:H layers, typically in the nm-thickness range. The minority-carrier density in the volume of the crystalline-silicon absorber is influenced by the quality of the interface between the a-Si:H and c-Si layers. For a solar cell, the density of interface defects determines the open-circuit voltage V_{oc} provided that the absorber itself or the poor back contact do not limit the minority-carrier density. Simulation studies identified a close relation between V_{oc} and the photoluminescence (PL) yield when the interface-defect density is varied [1-3].

We have shown that the electroluminescence (EL) yield is also affected by a poor front interface. Complementary to the drop in the open-circuit related PL yield with increasing interface-defect density, the EL yield also decreases [4]. In fact, the increase in the dark-current density with increasing interface-defect density N_{if} shifts the current-voltage characteristics under illumination so that the decrease of V_{oc}, the increase of saturation current density j_s and the decrease of the EL-yield are related. With V_{oc} in the range of 700 mV we demonstrated that the EL quantum efficiency can be as high as 0.13% [5]. In this paper we critically recall how the EL spectrum is constructed and compare our results with simulation results in the literature [6]. We then elaborate on the temperature dependence of the electroluminescence properties of the silicon devices, in particular for different N_{if}.

2 Theory The spectral luminescence photon flux from the solar cell can be described by Planck's generalised law [7]. Under the assumption that the free-carrier electron and hole densities can be expressed by quasi-Fermi levels E_{Fn} and E_{Fp} and for constant quasi-Fermi level splitting in the absorber, $E_{Fn}-E_{Fp}$, the emitted photon flux into the hemisphere reads approximately [7,8]

$$\mathrm{d}j_\gamma(\hbar\omega) = \frac{(\hbar\omega)^2}{4\pi^2\hbar^3c^2} A(\hbar\omega)\mathrm{e}^{\frac{E_{Fn}-E_{Fp}}{kT}}\mathrm{e}^{-\frac{\hbar\omega}{kT}}\mathrm{d}(\hbar\omega), \qquad (1)$$

where A is the absorptivity, determined by the optical properties of the solar cell and c is the velocity of light.

For analytical approximations with respect to EL, Würfel [8] noted that for a good luminescent pn diode the E_{Fn}–E_{Fp} is constant in the absorber from which the luminescence originates. Thus the applied voltage V_a equals $(E_{Fn}–E_{Fp})/e$ ($e = 1.6 \times 10^{-19}$ C). Thus from Eq. (1) it follows that [6,8]

$$\mathrm{d}j_\gamma(\hbar\omega) = \frac{(\hbar\omega)^2}{4\pi^2\hbar^3c^2} A(\hbar\omega)\mathrm{e}^{\frac{eV_a}{mkT}}\mathrm{e}^{-\frac{\hbar\omega}{kT}}\mathrm{d}(\hbar\omega)$$
$$= \frac{(\hbar\omega)^2}{4\pi^2\hbar^3c^2} A(\hbar\omega)\left(j_\mathrm{d}/j_\mathrm{s}\right)^m \mathrm{e}^{-\frac{\hbar\omega}{kT}}\mathrm{d}(\hbar\omega). \quad (2)$$

Here, j_d, the dark current density, and j_s are related to the emitted flux by a power law with diode ideality factor m.

3 Simulation details The simulation program SC-Simul was applied for the simulation of the luminescence experiments. It has been developed for a-Si:H/c-Si heterojunction and thin-film solar cells [9,10] and solves the continuity equations for electrons and holes and Poisson's equation. From the numerical solution, i.e., E_Fn and E_Fp, the luminescence photon flux can be calculated with Eq. (1). For non-constant quasi-Fermi level splitting the spatial generation profile of the luminescence and the absorption of luminescence photons are taken into account [11], with data for absorption coefficient α from [12,13]. Parameter values were adapted to take account of their temperature dependences, e.g., an increase in the electron and hole mobilities with decreasing T, a T-dependent band gap $E_\mathrm{G}(T)$ and effective density-of-states in the conduction band, $N_\mathrm{C}(T)$, and valence band, $N_\mathrm{V}(T)$, and, importantly a T-dependent $\alpha(T)$ that results in a T-dependent $A(\hbar\omega,T)$.

4 Simulation results

4.1 Shape of the EL spectrum Here we clarify how a typical EL spectrum looks like. Eq. (1) describes the EL spectrum by (i) the spectral dependence of A and (ii) the exponential term $\exp\left(-\hbar\omega/\left(kT\right)\right)$. A typical experimental EL spectrum from 300-µm a-Si:H/c-Si diode in Fig. 1 can be matched with the analytical expression of Eq. (1). In addition the full symbols represent a spectrum calculated with the approach in AFORS-HET [6] with α instead of A in Eq. (1). The expression with α represents the radiative recombination in a volume element but does not take into account photon propagation and outcoupling. The spectrum based on α shows the typical shoulder from the phonon-mediated transition but this feature is suppressed in a 300-µm solar cell in which the high-energy photons get largely absorbed. It can be concluded that a reliable calculation of the EL spectrum needs the A-term. The discussion in [6] on the EL spectra simulated with the α-term is thus not really applicable because the discussed spectra do not represent the emitted flux from a solar cell device but underestimate absorption of luminescence photons. In addition, the T-dependent EL spectra in [6] were calculated with a T-independent α so that e.g. the spectral width is not truly represented.

4.2 Inhomogeneous carrier distributions The EL spectrum is also determined by the distributions of the excess carrier densities or $E_\mathrm{Fn}(z)$–$E_\mathrm{Fp}(z)$ where z is the depth coordinate. Fig. 2 illustrates simulation results from SC-Simul for a 200-µm thick (n)a-Si:H/(p)c-Si diode with two different back-surface recombination velocities with emission to the left-hand side. The difference in the quasi-Fermi levels (a) translates into a lower emitted photon flux (b) for the inhomogeneous distribution. Only at the highest photon energies the emitted photon fluxes become comparable. It is noted that the integrated EL photon flux decreases from 2.35×10^{19} m^{-2} s^{-1} to 1.35×10^{19} m^{-2} s^{-1}. The applied voltage corresponds to $E_\mathrm{Fn} - E_\mathrm{Fp}$ at the junction on the left-hand side in Fig. 2(a) and the high-energy regimes ≥ 1.3 eV of the EL spectra in Fig. 2(b) can be evaluated with Eq. (1) to determine their values (about 550 meV)–despite the spectral differences.

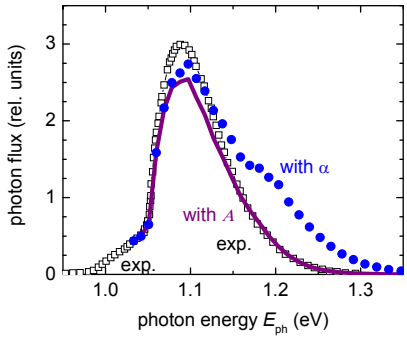

Figure 1 Comparison of EL spectra: experimental spectrum, digitized from Fig. 4 of [6] (open symbols) and analytical spectrum according to Eq. (1) (line). The dotted spectrum was calculated with the concept implemented in AFORS-HET. After [6,14].

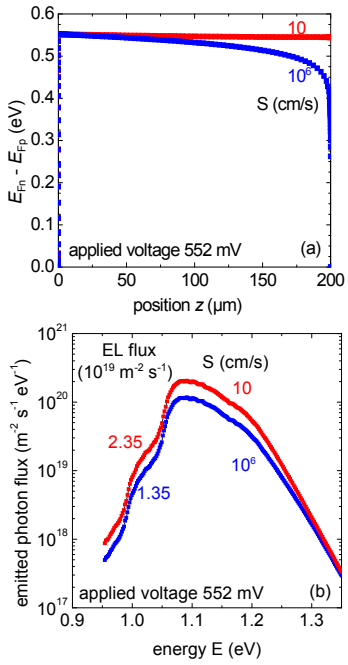

Figure 2 Spatial distribution of the free-carrier densities in terms of quasi-Fermi level splitting for high and low S at the back (a). The heterojunction with an n-type a-Si:H layer is on the left. Resulting EL spectra for emission into the left hemisphere. The integrated EL photon flux is indicated (b).

4.3 Temperature dependence of the EL spectrum Figure 3 displays 4 simulated EL spectra for high and low N_{if} at 195 K and at 300 K. The temperature can be identified in the high energy range of the spectrum with the higher slope for the 195 K case. The range of the low-energy is limited by the available data of α. The case with $N_{if} = 5 \times 10^6$ cm^{-2} represents a high-quality "model" interface. It can be seen that the 300 K emission decreases by almost a factor of 10 for $N_{if} = 5 \times 10^{12}$ cm^{-2}. At 195 K, the decrease in EL signal is much higher for the change in N_{if}.

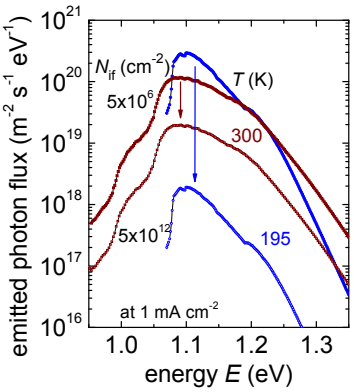

Figure 3 EL spectra for high and low N_{if} at 195 K and 300 K. The steeper slope at energies > 1.25 eV identifies the 195 K data.

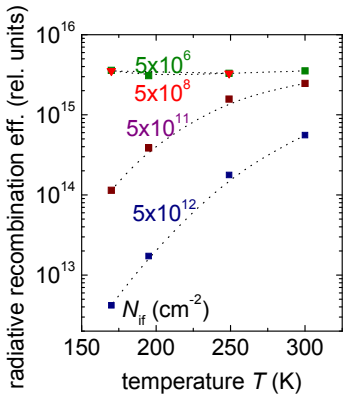

Figure 4 Spatially integrated radiative recombination rate for a range of high and low N_{if} at T between 170 K and 300 K. A decrease in EL with decreasing T is indicative of a higher N_{if}.

Inspection of the spectral variations in Fig. 3 shows a decrease in emission over the whole energy range for higher N_{if}, in contrast to Fig. 2. Thus Fig. 3 indicates that the increase in N_{if} does not change the spatial variations of the carrier distributions. This is in contrast to a variation at the back interface as was illustrated in Fig. 2 in which the back-interface related recombination leads to an inhomogeneous emission profile.

The EL-spectra difference, determined at the same dark-current level, is related to a variation in j_s according to Eq. (2) or to V_a. At the higher N_{if}, j_s increases. A lower V_a is needed to maintain the same injection current. As V_a is related to E_{Fn}–E_{Fp} a reduced EL emission flux results.

More data in Fig. 4 in terms of the radiative recombination rate in the solar cell show a clear distinction for the low N_{if} case and high N_{if} case. Here, the higher N_{if}, the stronger the decrease in radiative recombination rate and thus EL emission with decreasing temperature. The simulation results indicate that EL emission and its T-dependence can be a good indicator for interface quality.

5 Conclusions We have analysed the EL spectrum from (n)a-Si:H/(p)c-Si diodes with its energy dependence, related to A and the exponential Boltzmann-like term. The A-term correctly takes into account absorption of the luminescence photons, which the emission from a volume element, related to α and not to A, does not. Some earlier simulation results in [6,12] should thus be re-evaluated. Our simulations of the T-dependence of the EL have shown that it can be used as an indicator for the interface quality: a pronounced decrease of simulated EL flux with decreasing T is indicative for poor interface quality whereas a good interface results in an almost T-independent EL emission. The method can be exploited in combination with experiment and simulation to reveal more details about the interface-recombination properties.

Acknowledgements Travel support from the EWE-Stiftung, Oldenburg, is gratefully acknowledged.

References

[1] S. Tardon, M. Rösch, R. Brüggemann, T. Unold, G.H. Bauer, J. Non-Cryst. Solids **338**, 444 (2000).
[2] G.H. Bauer, R. Brüggemann, M. Rösch, S. Tardon, T. Unold, Phys. Status Solidi C **1**, 1308 (2004).
[3] K. v. Maydell, H. Windgassen, W. A. Nositschka, U. Rau, P. J. Rostan, J. Henze, J. Schmidt, M. Scherff, W. Fahrner, D. Borchert, S. Tardon, R. Brüggemann, H. Stiebig, M. Schmidt, Proc. 20th Europ. Photovoltaic Solar Energy Conference, Barcelona, Spain, 2005 (WIP, Munich 2005), p. 822.
[4] R. Brüggemann, J. Behrends, S. Meier, S. Tardon, J. Optoelectron. Adv. Mater. **9**, 77 (2007).
[5] R. Brüggemann and S. Olibet, Energy Proc. **2**, 19 (2010).
[6] W. Fuhs, A. Laades, K. von Maydell, O.B. Gusev, E. Terukov, S. Kazitsyna-Baranovski, G. Weiser, J. Non-Cryst. Solids **352**, 1884 (2006).
[7] P. Würfel, J. Phys. C **15**, 3967 (1982).
[8] K. Schick, E. Daub, S. Finkbeiner, P. Würfel, Appl. Phys. A **54**, 109 (1992).
[9] M. Rösch, R. Brüggemann, G.H. Bauer, 2nd World Conference on Photovoltaic Solar Energy Conversion, Vienna, Austria, 1998 (Joint Research Centre, Ispra, 1998), p. 946.
[10] M. Rösch, T. Unold, R. Pointmayer, G.H. Bauer, MRS. Symp. Proc. **557**, 463 (2000).
[11] R. Brüggemann, Philos. Mag. B **89**, 2519 (2009).
[12] M.A. Green, M.J. Keevers, Progr. Photovoltaics **3**, 189 (1995).
[13] G.G. McFarlane, T.P. MacLean, J.R. Quarrington, V. Roberts, Phys. Rev. **111**, 1245 (1958).
[14] G. Weiser, S. Kazitsyna-Baranovski, R. Stangl, J. Mater. Sci.: Mater. Electron. **18**, S93 (2007).

